Multi-dimensional numerical analysis on ignition and extinction phenomena in the heated micro channel

Keisuke Akita[1], Youhi Morii[1], Hisashi Nakamura[1], Takuya Tezuka[1], Kaoru Maruta[1,2]
[1]Institute of Fluid Science, Tohoku University, Sendai, Miyagi, Japan
[2]Far Eastern Federal University, Russky Island, Russia

1 Introduction

Research on the ignition characteristics plays an important role in the development of high-efficiency internal combustion engines. To obtain basic information for the development, The use of micro flow reactor with a controlled temperature (MFR) as the combustion test methods has experimental advantages for quickly acquiring data and numerical advantages for the small computational domain compared with the conventional ignition testing methods. In MFR, which is composed of a heated quartz tube having less than quenching diameter, three types of flames are observed depending on the inlet velocity [1–3]. Stable normal flame in a high inlet velocity regime and stable weak flame in a low inlet velocity regime have been observed. In the intermediate inlet velocity regime between normal and weak flames, Flames with Repetitive Extinction and Ignition (FREI) have been observed. In FREI condition, a flame which ignites at higher wall temperature region (downstream) propagates upstream and is extinct at lower wall temperature region (upstream) because of the large surface-to-volume ratio in the quenching diameter tube. After the flame extinction, the fresh mixtures flow downstream by convection and is self-ignited again by the heat from hot wall temperature. Recently, Lapointe et al. [4] conducted the numerical study of FREI with fuels relevant to internal combustion engines and show that low-temperature chemistry effects on the ignition in MFR. Focusing on a minimum hydrocarbon fuel, CH_4, Ayoobi et al. [5] investigated flame instabilities in narrow channels for various tube diameters and equivalence ratio using two-dimensional numerical simulation. Miyata et al. [6] evaluated FREI and oscillating flame with total heat transfer rate analysis based on the three-dimensional Direct Numerical simulation (DNS) results at the stoichiometric CH_4/air conditions. Although DNS of CH_4/air FREI have been conducted, the ignition and extinction mechanisms in MFR considering multi-dimension has not been investigated. Nakamura et al. [7] conducted one-dimensional numerical simulation with a constant Nusselt number for stoichiometric CH_4/air FREI and indicates bifurcated flame propagate downstream against the main flame propagating direction (upstream) with chemical analysis. However, the simulation assuming the constant Nusselt number is not fully accurate because the gas temperature is much higher than the wall temperature. Therefore, this study aims to clarify the ignition and extinction phenomena of FREI in consideration of multi-dimensional effects using the two-dimensional numerical simulation of stoichiometric CH_4/air FREI.

2 Nunerical setup

2.1 Numerical Methods and conditions

To clarify the multi-dimensional effects on FREI in MFR, the axial symmetry the two-dimensional numerical simulation was conducted. Incompressible Navier-Stokes equations were solved by using reactingFoam of OpenFOAM. Computational geometry and mesh is shown in Fig. 1. The computational domain is set to 100 mm in the flow direction and 1 mm in $r-$direction. 8000 meshes were used at $x-$direction and 100 meshes were used at $r-$direction. The boundary condition of wall temperature was given by the hyperbolic tangent formula following

$$T_{\mathrm{w}}(x) = \frac{T_{\max} - T_0}{2} \tanh(\alpha x + \beta) + \frac{T_{\max} + T_0}{2} \tag{1}$$

where $T_{\max} = 1350$ K, $T_0 = 300$ K, $\alpha = 0.821$ and $\beta = -4.20$. Coefficients α, β is determined by the experimental wall temperature profile. Numerical conditions were based on our experiment. Methane/air mixture at the equivalence ratio of 1 and inlet velocity of 15 cm/s under atmospheric pressure was used. GRI-Mech 3.0 [8] was used as detailed chemical kinetics. The flame position was defined as the peak location of the heat release rate (HRR) profile.

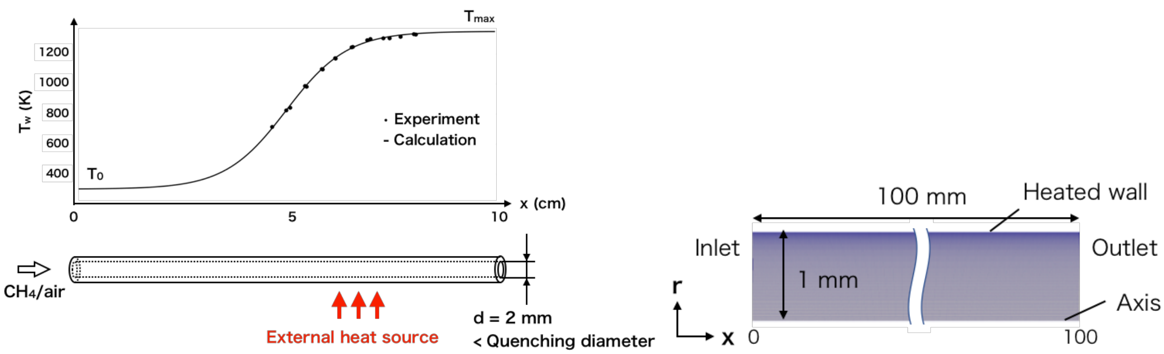

(a) Schematic of MFR. (b) Computational domain in MFR.

Figure 1: Numerical setup.

2.2 Validation and verification

The numerical simulation with 12000 meshes at $x-$direction was conducted to verify the numerical accuracy. Grid convergence of 8000 grid case in x-direction was confirmed by the correspondence of the ignition position, extinction position and cycle frequency of FREI with 12000 grid case. To validate two-dimensional simulation, the experimental shooting result of FREI by CCD camera is shown in Fig. 2 (a) and numerical results of FREI heat release rate are shown in Fig. 2 (b). Simulations were able to qualitatively reproduced curved shapes of the flames in the experiments. From the next results section, same time history as Fig. 2 (b) is used.

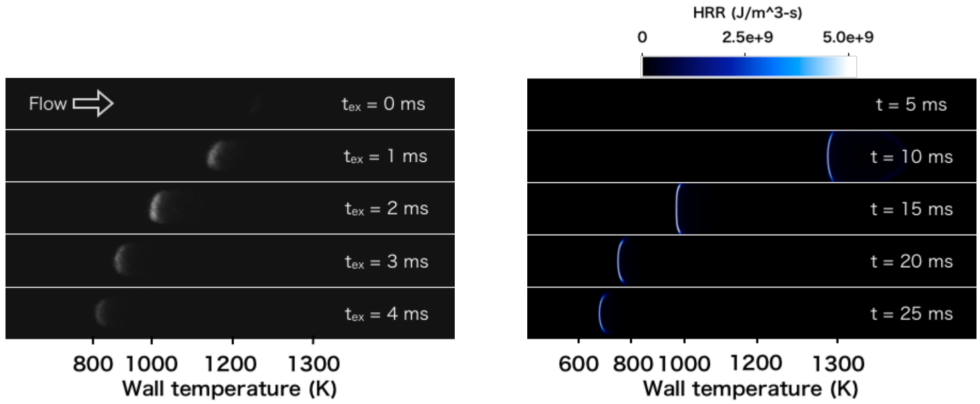

(a) Experimental images of FREI. (b) Heat release rate distributions of FREI.

Figure 2: Comparison of Flame shapes between the experiment and two-dimensional simulation.

3 Results and discussion

3.1 Overall two-dimensional FREI mechanisms

At first, the overall dynamics of FREI were discussed. As indicated the previous section in Fig. 2, the self-ignited flame propagates upstream and extincts at a low-temperature region. To understand the behavior of flames in detail, the first largest and second largest peaks of heat release rate at the central axis of the tube are extracted. In this numerical results, two kinds of one cycle results with and without flame bifurcation are obtained in spite of the same ignition location, extinction location and frequency in each cycle after ten cycle simulations. In this study, to compare the results with one-dimensional simulations by Nakamura et al. [7], flame bifurcation cases are selected. The peaks of heat release rate at $r = 0$ mm are plotted in Fig. 3.

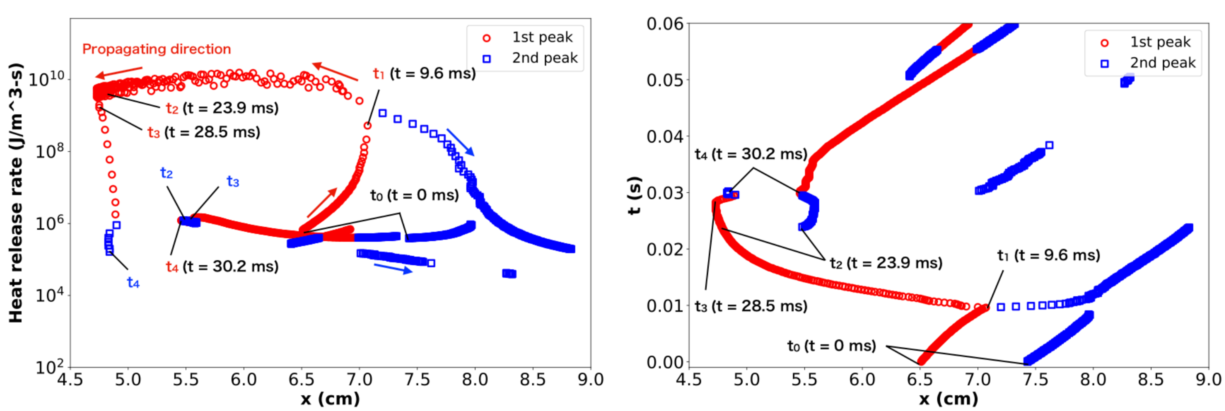

(a) Peaks value of heat release rate against the locations. (b) x-t at the heat release rate peaks.

Figure 3: The history of the heat release rate peaks on the central axis.

Figure 3 (a) presents the largest and second largest peak values of heat release rate against locations of peaks. Figure 3 (b) presents the relationship between time and the location of the heat release rate peaks.

The arbitrary time of the before ignition is set to initial time t_0 ($t = 0$ ms) to consider the entire ignition phenomenon. In Fig. 3 (a) from $t = t_0$ to t_1, two small HRR peaks move downstream by the convection. As the increase of heat transfer from wall to gas, the 1st peaks of heat release rate gradually increase. After mixture at the boundary between the fresh and burnt mixture is self-ignited at $t = t_1$, the 1st peaks of heat release rate shifts upstream, while bifurcated 2nd largest peaks of heat release rate shifts downstream and gradually decreases in the lean fuel condition in downstream. This bifurcated flame has been confirmed also by one-dimensional numerical simulations [7]. When 1st peaks of heat release rate reach to around $x =$ 4.77 cm at $t = t_2$, 2nd peaks of heat release rate appear around $x = 5.5$ cm before the main flame is extinct. After $t = t_3$, 1st peaks of heat release rate immediately decrease while shifting slightly downstream and disappear at $t = t_4$ Around the extinction of flame from $t = t_2$ to t_4, separated two peaks of heat release rate is observed. After the disappearance of peaks at the upstream side at $t = t_4$, the 1st peak of heat release rate flowing downstream at the boundary between the fresh and burnt mixture lead to next cycle ignition. In the next section, multi-dimensional characteristics of these heat release peaks especially around the ignition and the extinction are investigated in detail.

3.2 Ignition phase

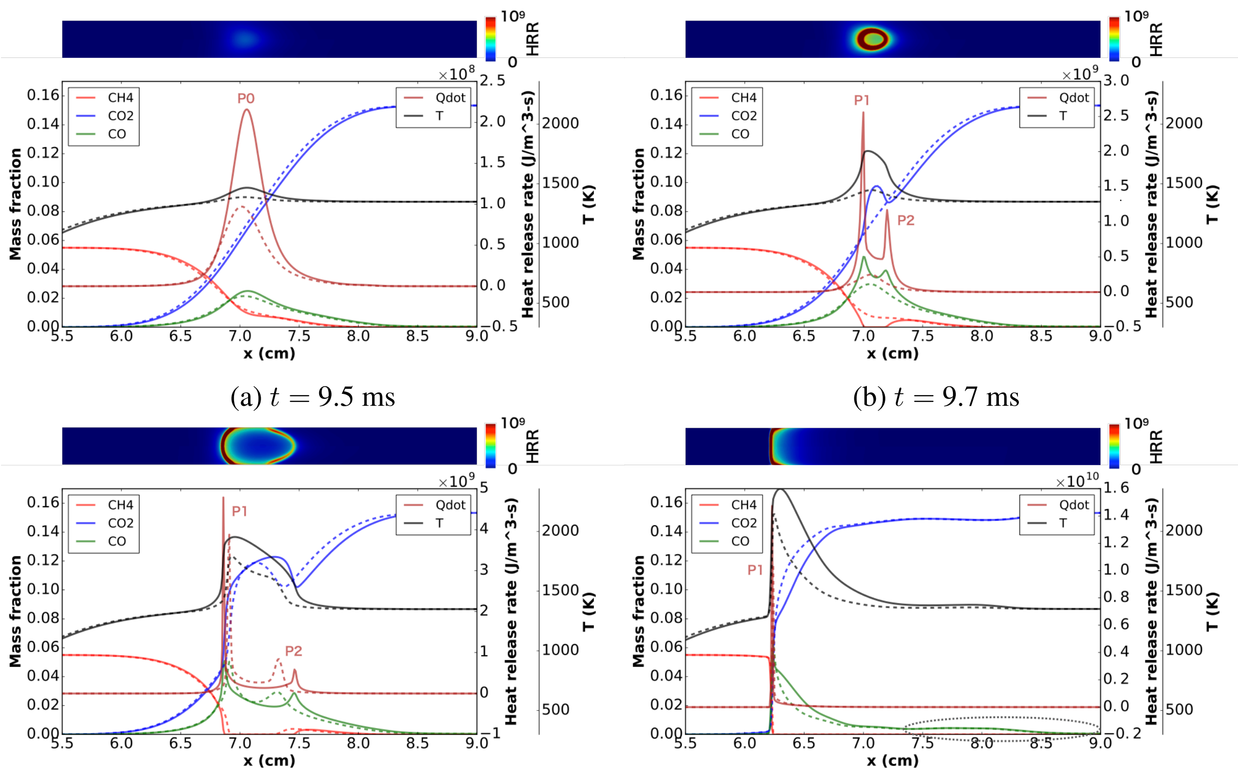

(a) $t = 9.5$ ms (b) $t = 9.7$ ms

(c) $t = 9.9$ ms (d) $t = 12.0$ ms

Figure 4: Distributions of heat release rate and profiles of mass fraction, heat release rate and temperature at r = 0 (solid line), 0.75 mm (dotted line) in ignition phase.

To reveal the ignition mechanisms in consideration of multi-dimensional effects, two-dimensional distributions of heat release rate and profiles of mass fractions of primary species, heat release rate and temperature at $r = 0$ mm (solid line), 0.75 mm (dotted line) were shown as Fig. 4. In Fig. 4 (a) at the initiation of the ignition, the heat release rate peak (P0) at $r = 0$ mm is larger than that at $r = 0.75$ mm. These results indicate as far as this computational conditions are concerned, the mixture at the central axis is more ignitable conditions than at the wall side. Figure 4 (b) represents P0 at $r = 0$ mm is bifurcated to P1 and P2, whereas only one peak of the heat release rate is obtained at $r = 0.75$ mm. After the ignition kernel appearing in Fig. 4 (a) spread spherically, the flame shown in 4 (b) become circle stretched in flow direction. At $r = 0$ mm and $x = 7.1$ cm in the circle of flame, reactant CH_4 is consumed and product CO2 is produced In Fig. 4 (c), flame propagating from the ignition kernel in the r-direction is immediately extinct and flame are separated to main flame (P1) propagating upstream and bifurcated flame (P2) propagating downstream. As shown in Fig. 4 (d) the bifurcated flame is extinct because of propagating into mixture in the fuel lean condition in downstream. The peak of bifurcated heat release rate (P2) the decrease with decrease of CO mass fraction.

3.3 Extinction phase

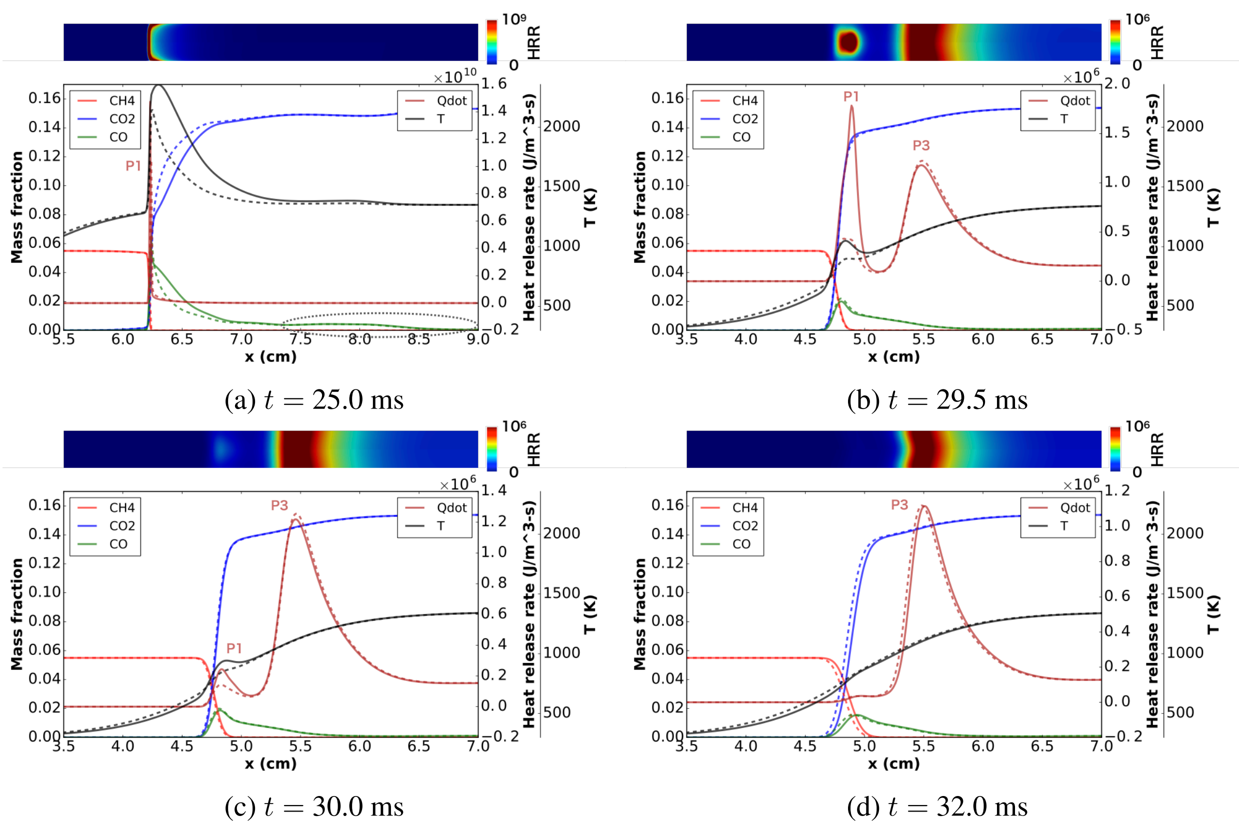

(a) $t = 25.0$ ms (b) $t = 29.5$ ms (c) $t = 30.0$ ms (d) $t = 32.0$ ms

Figure 5: Distributions of heat release rate and profiles of mass fraction, heat release rate and temperature at $r = 0$ (solid line), 0.75 mm (dotted line) in extinction phase.

To examine the extinction in detail, two-dimensional distributions of heat release rate and profiles of mass fraction, heat release rate and temperature at $r = 0$ (solid line), 0.75 mm (dotted line) were shown as Fig. 5. In Fig. 5 (a) , the flame having the largest peak of heat release rate (P1) propagetes upstream and is extinct by the heat loss to the wall. As shown in Fig. 5 (a), (b) and (c), before the flame is extinct, the other peak of heat release rate (P3) appears. P3 is produced by the remaining CO which not react while main flame propagate in Fig. 5 (a). Spatially separated two peaks of heat release rate in the extinction phase have been reported in the one-dimensional simulation with constant Nusselt number [7]. However, the distance between the peaks is very small, about 1mm in the one-dimensional simulation. The distance of about 1 cm on this two-dimensional simulation is much larger than one-dimensional simulation. The reason is that heat loss at the central axis is smaller than in the wall side in the two-dimensional simulation. In Fig. 5 (d), P1 disappears and the P3 flows downstream.

4 Conclusions

Axial symmetry two-dimensional numerical simulation of stoichiometric CH_4/air FREI was conducted and the ignition and extinction phenomena in MFR was investigated in detail. In the ignition phase, the ignition occurs at the central axis of the tube and the flame is separated to the opposite direction. In the extinction phase, the distance of two heat release peaks which produced from CO reaction is larger than that of one-dimensional simulation.

References

[1] Maruta K, Kataoka T, Kim N, Minaev S, Fursenko R. (2005). Characteristics of combustion in a narrow channel with a temperature gradient. Proc. Combust. Inst. 30: 2429.

[2] Tsuboi Y, Yokomori T, Maruta K. (2009). Lower limit of weak flame in a heated channel. Proc. Combust. Inst. 32: 3075.

[3] Yamamoto A, Oshibe H, Nakamura H, Tezuka T, Hasegawa S, Maruta K. (2011). Stabilized three-stage oxidation of gaseous n-heptane/air mixture in a micro flow reactor with a controlled temperature profile. Proc. Combust. Inst. 33: 3259.

[4] Lapointe S, Druzgalski CL, McNenly MJ. (2018). Numerical study of a micro flow reactor at engine pressures: Flames with repetitive extinction and ignition and simulations with a reduced chemical model. Combust. Flame, 197: 102.

[5] Ayoobi M, Schoegl I. (2017). Numerical analysis of flame instabilities in narrow channels: Laminar premixed methane/air combustion. Spray Combust. Dynamics. 9: 155.

[6] Miyata E, Fukushima N, Naka Y, Shimura M, Tanahashi M, Miyauchi T. (2015). Direct numerical simulation of micro combustion in a narrow circular channel with a detailed kinetic mechanism. Proc. Combust. Inst. 35: 3421.

[7] Nakamura H, Fan A, Minaev S, Sereshchenko E, Fursenko R, Tsuboi Y, Maruta K. (2012). Bifurcations and negative propagation speeds of methane/air premixed flames with repetitive extinction and ignition in a heated microchannel. Combust. Flame, 159: 1631.

[8] Smith GP, Golden DM, Frenklach M, Moriarty NW, Eiteneer B, Goldenberg M, Bowman CT, Hanson RK, Song S, Gardiner Jr. WC, Lissianki V, Quin Z. (2002).